

OPTIMIZATION OF TRAIN DETECTION IN INTELLIGENT RAILWAY TRANSPORTATION SYSTEMS

Patricio Donato, Jesús Ureña, Manuel Mazo, Juan Jesús García, Álvaro Hernández, Fernando Álvarez

*Departamento de Electrónica, Escuela Politécnica, Universidad de Alcalá
Carretera a Barcelona, km. 33.6 – Alcalá de Henares – CP:28871 – Madrid – Spain
Tel: +34918856592 / Fax: +34918856591
e-mail: donatopg@depeca.uah.es*

Abstract: The reliable detection of trains in intelligent transportation systems is very important for a safe circulation. The system proposed makes the detection with a sensor located next to the railway, without additional electronics in this place. All the electronic process equipment is concentrated in a point that can be far away the rail. Moreover, the system is capable to detect the sense of circulation. Several sensors can be connected to the process equipment with only two wires. In order to compensate the attenuation and external noise, a signal coded with Golay complementary sequences is used.

Keywords: Sensors, Train detection, intelligent transportation systems, Localisation.

1. INTRODUCTION

Now, the developments on security and traffic control are one of the high-priority lines of R+D in the railway scope (OPTI, 1999). In the automation of the railway traffic circulation it is very important to have reliable detectors of passage of trains on certain points, especially in the junctions of the routes. The existing commercial electronic wheel detectors in the market are based on RLC circuits placed next to the rail and tuned in a fixed frequency of the tens of kHz. In a normal condition (when the rail is free), a constant current in module and phase circulates in the RLC circuit. When the train wheel is above the detector, the inductance experiences a change in its magnitude, due to variations of magnetic permeability and magnetic flux density in its surroundings. Also, the change in the inductance modifies the impedance of the RLC circuit, which causes variations in the current, easily measurable.

In (Futsuhara, 1988, 1999) is proposed the realisation of a fail safe wheel train detector using two coils working as emitter and receiver respectively. The detector senses the wheels as changes in the magnetic coupling between the coils placed at either rail sides. The coils are installed in the same plane with parallel axes and over a metal plate, and the emitter coil is excited with a harmonic current.

In other systems with two pairs of coils (emitter and receiver) a code is processed in a continuous way. The system described in (Ureña, 2001) is based on the magnetic flux codification with a 13-bit Barker code. Being interrupted by the passage of a train wheel detects its presence. The received signal is correlated with the Barker code. This process takes

advantage of the 13-bit Barker code properties, as the autocorrelation function with a very marked peak with a 13:1 amplitude ratio respect of the lateral lobes. This property allows to distinguish the Barker code making the correlation between the received signal and the transmitted one, in spite of the external noise or the attenuation of the channel. The problem of the Barker codes is their maximum limit of 13 bits that limits the SNR that can be tolerated in the system.

The typical exigencies to these systems are (RENFE, 1999):

- The detection point will consist of two inductive detectors heads mounted on the rail and an electronic unit of route composed of the necessary elements which they'll provide a safe interface with the central process unit.
- The outer equipment will fulfil the norm of maximum height until a determined distance. The sensor coils will have to be below the maximum altitude of the rail (this is represented in fig. 1).
- The system will correctly work with trains in movement and speeds between 0 and 300 Km/h
- The equipment must be immune to external interferences, such as atmospheric discharges, returns of traction system until 2000A at 3kV of DC, and 500A at 25 kV of AC with trains with conventional systems or integral commutators, as well as to the braking systems of the trains.
- The outer equipment will have to have designed characteristics to exclude the inadequate operation due to mechanical vibrations or any other outer forces.
- The external equipment will work at temperatures from -40°C to +80°C, with a humidity of 90%.

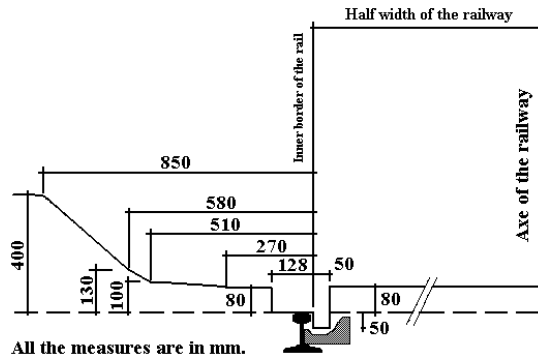


Fig. 1: Norm of maximum height in the railway.

From all this, it is deduced that one of the most important aspects is that the system must be designed guaranteeing great immunity to the noise. In the present work we propose a detection system based in the use of two pairs of emitter (TX) and receiver (RX) coils in each detection point. These two pairs of coils are part of an AC bridge and are interconnected between them. Besides, we'll move away the electronic process unit to the location of the control unit (located inside technical buildings). For that reason, the proposed solution is based on the emission of a coded signal generated from Golay complementary sequences. The implementation of the correlation can be made in systems of reprogrammable logic (Hernández, 2002), by means of efficient Golay correlators (Popovic, 1999). With this technique, aside from compensating the signal fall in the wires, immunity to the interferences is obtained. It means that the signals can be captured in presence of noise of the same frequency that the one used in the modulation. Moreover, in this work we propose the detection of the direction of the circulation using the same sensor system, and we consider to extend the sensor system from two pairs of coils to "n" pairs of coils distributed in several detection points. Following up the research, the most critical aspects of the system will be studied: the location of the coils, the design of the sensor system, and the process of the coded signals.

2. STUDY OF THE LOCATION OF THE COILS

The location of the coils is very important because we will design the sensor and the signal conditioner according to it. Its study was done by means of a specific software for Finite Element Analysis (FEA). Originally the analysis was carried out in two dimensions (2D), using Quickfield 5, but then it was improved in three dimensions (3D), using ANSYS 6.1 (Ansys, 2002). With this software we can analyze and calculate the magnetic field strenght, the flux density and other electromagnetic magnitudes in the surroundings of the rail. The procedure to make the analysis can be resumed as follows:

- Design of a geometric model with all the elements that compose the system: rail, emitter and receiver coils, and wheel train.

- Definition of the magnetic properties of the materials, and the physical parameters of the emitter coil, (current density, shape and size).
- Generation of the mesh to divide the continuous system in a set of continuous elements.
- Set of boundary conditions (Flux normal and parallel).
- Solution of the system and post-process of the output data.

In order to understand this study about the coils, we organize it specifying all the degrees of freedom or design variables that are contemplated:

- Position of both coils.
- Orientation of both coils.
- Magnetic link between each coil and the rail.
- Size and shape of each coil.
- Number of turns and current intensity in the emitter coil.

Due to there are many degrees of freedom, we must fix some of them. The parameters related to the design of the coils (size, shape, turns and current) were taken from a previous work (Donato, 2003a, 2003b). These parameters (see table 1a) have a direct relation with the magnitude of the density of flux, B, and with the induced voltage in the receiver coil. However, they do not have influence in the relative variation in the field B when the rail is free and when is occupied (if we consider the magnetic permeability linear). About the position, we use the maximum heights imposed by the norm (fig.1) (RENFE, 1999), and we can only change the distance between TX coil and the rail. So, our study was concentrated on the distance and orientation of the coils, besides the magnetic link of each one. In table 1b the used options are resumed, and in fig.2 they are represented in a 2D view of the rail. In table 2 and 3 the results of the simulations corresponding to these values are resumed, taking into account if the wheel is present. The relative attenuation ΔB is the ratio between the flux density B when the wheel is present and when the rail is free. To get a good detection of the wheel, it is convenient to have a high attenuation ratio.

Table 1a: Fixed parameters

Parameter	Shape	Radius	Height	Turns
RX Coil	Cylinder	2 cm	4 cm	400
TX Coil	Cylinder	0,5 cm	4 cm	200

Table 1b: Variable parameters

Parameter	Values
Angle of TX	0°; 22.5°; 45°
Angle of RX	0°; 22.5°; 45°
Magnetic link of TX	Iron ($\mu=4000$); air ($\mu=1$)
Magnetic link of RX	Iron ($\mu=4000$); air ($\mu=1$)
Distance TX-Rail	0; 1.5cm

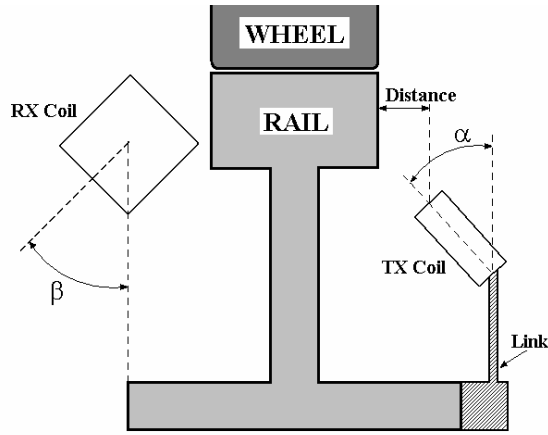


Fig. 2: Design parameters.

Table 2: Results of the simulations with a distance between emitter coil and rail of 0 cm

α (°)	β (°)	Link(TX/RX)	Wheel	B (T)	ΔB (rel.)
0	0	Iron / Air	Not	7.48E-8	5.45
0	0	Iron / Air	Yes	1.37E-8	
0	0	Air / Air	Not	1.86E-8	1.46
0	0	Air / Air	Yes	1.28E-8	
0	0	Iron / Iron	Not	2.25E-7	2.07
0	0	Iron / Iron	Yes	1.08E-7	
0	22.5	Iron / Air	Not	7.77E-8	5.23
0	22.5	Iron / Air	Yes	1.48E-8	
0	22.5	Air / Air	Not	1.32E-8	0.82
0	22.5	Air / Air	Yes	1.60E-8	
0	45	Iron / Air	Not	7.79E-8	3.89
0	45	Iron / Air	Yes	2.00E-8	
0	45	Air / Air	Not	2.64E-8	1.17
0	45	Air / Air	Yes	2.26E-8	
22.5	0	Iron / Air	Not	1.54E-7	8.99
22.5	0	Iron / Air	Yes	1.71E-8	
22.5	0	Air / Air	Not	2.50E-8	1.9
22.5	0	Air / Air	Yes	1.32E-8	
22.5	0	Iron / Iron	Not	2.97E-7	1.9
22.5	0	Iron / Iron	Yes	1.57E-7	
22.5	22.5	Iron / Air	Not	1.35E-7	6.7
22.5	22.5	Iron / Air	Yes	2.01E-8	
22.5	22.5	Air / Air	Not	2.35E-8	1.44
22.5	22.5	Air / Air	Yes	1.64E-8	
22.5	45	Iron / Air	Not	1.23E-7	5.68
22.5	45	Iron / Air	Yes	2.16E-8	
22.5	45	Air / Air	Not	3.32E-8	1.88
22.5	45	Air / Air	Yes	1.77E-8	
45	0	Iron / Air	Not	1.20E-7	5.98
45	0	Iron / Air	Yes	2.01E-8	
45	0	Air / Air	Not	5.39E-8	3.41
45	0	Air / Air	Yes	1.58E-8	
45	0	Iron / Iron	Not	2.67E-7	1.76
45	0	Iron / Iron	Yes	1.52E-7	
45	22.5	Iron / Air	Not	1.02E-7	3.61
45	22.5	Iron / Air	Yes	2.82E-8	
45	22.5	Air / Air	Not	5.49E-8	2.39
45	22.5	Air / Air	Yes	2.30E-8	
45	45	Iron / Air	Not	9.70E-8	4.1
45	45	Iron / Air	Yes	2.37E-8	
45	45	Air / Air	Not	4.94E-8	2.25
45	45	Air / Air	Yes	2.19E-8	

Table 3: Results of the simulations with a distance between emitter coil and rail of 1.5 cm and RX coil without magnetic link

α (°)	β (°)	Link(TX/RX)	Wheel	B (T)	ΔB (rel.)
0	0	Iron / Air	Not	1.70E-7	14.13
0	0	Iron / Air	Yes	1.20E-8	
22.5	0	Iron / Air	Not	2.40E-7	12.74
22.5	0	Iron / Air	Yes	1.89E-8	
45	0	Iron / Air	Not	2.02E-7	11.11
45	0	Iron / Air	Yes	1.82E-8	

All the analysis was done in the same conditions. With these results, we verify and improve the results and conclusions obtained in (Donato, 2003a, 2003b). The first conclusion obtained is the necessity of a magnetic link between the TX coil and the rail. From table 3 can be seen the difference in ΔB when the TX coil is linked to the rail (Iron) and when not (Air). Under the same conditions, ΔB when the TX coil is not linked is lower than ΔB when the TX coil linked to the rail. The next conclusion about the coils is the RX coil does not need a magnetic link with the rail, because the ratio of attenuation ΔB turns lower. Other important inference from these analyses is the importance of the distance between the TX coil and the rail. Comparing the results from tables 2 and 3, it can see how ΔB is larger when TX coil is distanced 1.5 cm from the top border of the rail.

After analyzing and process all the results of the simulations of the different physical configurations (tables 2 and 3 are a condensed selection of data), it was chosen the location seen in fig. 3. The optimal location for the emitter coil is at 1,5 cm respect of the border of the rail and using the maximum height permitted by the norm (RENFE, 1999) (fig. 1). The inclination of the coil respect of the vertical axis can be from 0° to 22.5°, but we choose an angle of 0° for its better performance. Using the results of the simulations combined with the physical parameters of the coils (table 1a), it can be calculated the variations of magnetic flux in the RX coil. In fig. 4 it is represented the RX coil after the generation of the mesh, with the elements and nodes where is solved the system. All the nodes are distributed in the top and bottom areas, and between them.

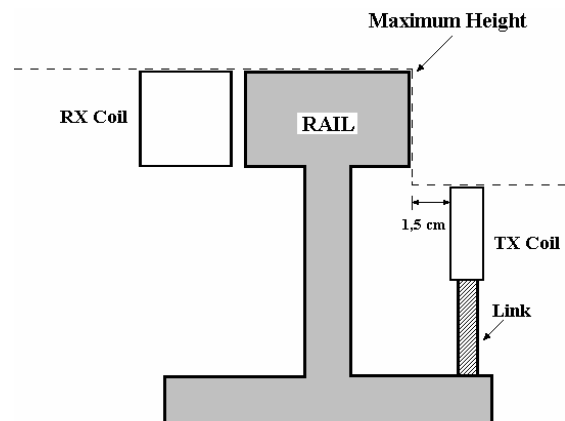


Fig. 3: Location of the emitter and receiver coils.

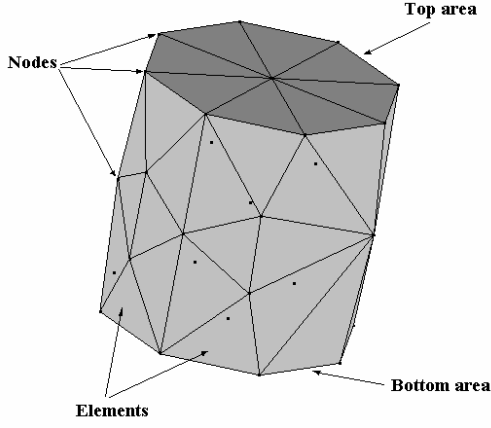


Fig. 4: RX coil meshed

The top and bottom areas are perfect planes, but the nodes between both areas form an irregular area which is almost plane, but not a perfect plane (to calculate the magnetic flux, this area is approximated to the others). In the table 4 are resumed the results of the magnetic flux calculation, as much for the free rail case (Φ_{rf}) as for the case in that passes a wheel of the train (Φ_w).

Table 4: Magnetic flux in the RX coil

Plane	Φ_{rf} (Wb)	Φ_w (Wb)	$\Delta\Phi$ (rel.)
Top	4.28E-10	3.03E-11	14.13
Middle	3.78E-10	3.01E-11	12.58
Bottom	3.51E-10	4.82E-11	7.29

The cause of the difference in the flux attenuation $\Delta\Phi$, from table 4, is the dispersion of the magnetic field, which trend to concentrate into the iron of the rail. Due to the position of the emitter coil, the magnetic field at the other side of the rail is more strength in the top area. Anyway, the average of flux attenuation is 11,33; this is 21 dB of attenuation in the received signal, which is a very good magnitude of attenuation to implement the sensor and apply the proposed signal process technique.

3. SENSOR SYSTEM

The two pairs of emitter and receiver coils studied in the previous section are part of an AC bridge (fig. 5). They are connected in series, with their homologous terminals connected in an opposite way. The particular AC bridge used is an implementation of the Maxwell bridge. All the components of the bridge (excepting the coils) are far away respect of the rail, and are included in the electronic process unit. When the system is in stationary condition (rail free), the bridge is balanced, and the voltage between the midpoints of the two branches is null. When the wheel of the train pass on the point where the coils have been placed, the coupling coefficient in the same ones falls. This variation in the coupling coefficient affects the total inductance of the branch, and causes that the bridge turns unbalanced. Then appears a differential voltage between the two branches which it has the same waveform that the coded signal of the input.

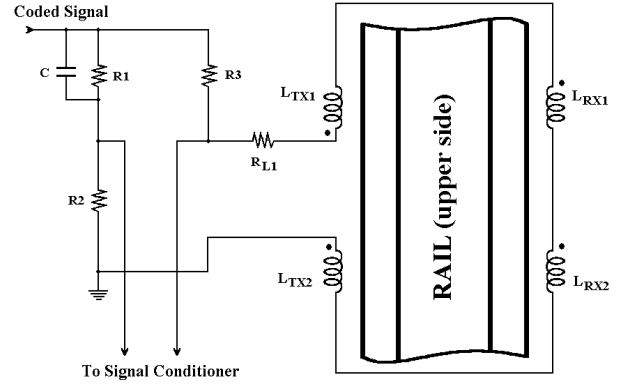


Fig. 5: AC bridge with the emitter and receiver coils.

Using the two pairs of coils connected like the fig. 5, the change in the total inductance (L_{total}) of the sense branch will be different according to which pair of coils is affected. The mathematical expression of L_{total} is:

$$L_{total} = L_{TX1} + L_{TX2} + L_{RX1} + L_{RX2} + 2M_1 - 2M_2 \quad (1)$$

$$M_X = k \cdot \sqrt{L_{TX} \cdot L_{RX}}$$

M_1 and M_2 are the mutual inductances of each pair of coils, which depends of the inductances of each coils and its coupling coefficient. So, L_{total} will changes of different way if the wheel train is above the pair of coils 1 or 2, because the influence of each pair of coils in the bridge is different. It is useful to know the direction of circulation of the train.

4. PROCESS AND CODIFICATION OF THE SIGNAL

4.1. Golay complementary sequences

Given a pair of Golay complementary sequences (a,b), of length N, constituted by values $\{-1, +1\}$, it is known that the sum of autocorrelations of both sequences of the Golay pair, C_{aa} and C_{bb} , gives an ideal result: a function delta of Dirac, $\delta(n)$, of weight $2N$, that is:

$$C_{aa} + C_{bb} = 2N\delta(n) \quad (2)$$

This is even fulfilled if the sequences are superposed (Tseng, 1972). That is to say, if two signals, A[n] and B[n], are generated:

$$\begin{aligned} A(n) &= a(n - n_1) + a(n - n_2) \\ B(n) &= b(n - n_1) + b(n - n_2) \end{aligned} \quad (3)$$

Then:

$$C_{Aa} + C_{Bb} = 2N\delta(n - n_1) + 2N\delta(n - n_2) \quad (4)$$

Where C_{Aa} and C_{Bb} represent the cross correlation between the signal indicated with the sub-index. It must be fulfilled that the separation between superposed sequences $(n_2 - n_1) > 0$.

4.2. Generation of the coded signal

We use a continuous coded signal emission, and a continuous signal process using the cross correlation (Donato, 2003a, 2003b). In particular, we use a specific sequence superposition of $N/2$ bits. The mathematical expression is:

$$\begin{aligned} A(n) &= \sum_k a(n - k \cdot N/2) \quad \forall k \\ B(n) &= \sum_k b(n - k \cdot N/2) \quad \forall k \end{aligned} \quad (5)$$

The result of the sum of correlations will be:

$$C_{Aa} + C_{Bb} = 2N \sum_k \delta(n - k \cdot N/2) + C_{na} + C_{nb} \quad (6)$$

In the previous expression it was assumed in the process a Gaussian noise (n), whose repercussion in the output comes given by $C_{na} + C_{nb}$. This contribution is, in terms of power, $2N$ times lower than the amplitude of the deltas.

The generated signals $A(n)$ and $B(n)$ with superposition $N/2$ have special characteristics:

- $A(n)$ and $B(n)$ are periodic signals of $N/2$ period.
- Within a period, half of the values of $A(n)$ and $B(n)$ are null.

Because half of the values is null, it is possible, with a simple displacement of one of them $N/4$ with respect to the other, to send them multiplexed in time for the same channel.

4.3. Implementation of the system

With the generated superposed sequences, the signal definitively sent to the emitter coil is modulated digitally, by means of a BPSK modulator, with a symbol constituted of two periods of an square signal of 50kHz. This way, the signal adapts to the central frequency of work wanted for the system. In addition, we use BPSK modulation because it has a narrow bandwidth. The block diagram of the system is in fig. 6 and includes different blocks:

- AC bridge with the sensor coils (TX and RX).
- A/D Converter (sampling frequency of 1 MHz).
- BPSK demodulator.
- Demultiplexer to reconstitute the order of the signals $A(n)$ and $B(n)$.
- Double correlator, C_{Aa} and C_{Bb} , and the sum of their outputs.
- Peak detector to recover the train of deltas.

As clock is arranged in the process equipment, as much to the emission as for the reception, the demodulation can be made synchronously. So the typical sidelobes of the asynchronous detection are avoided

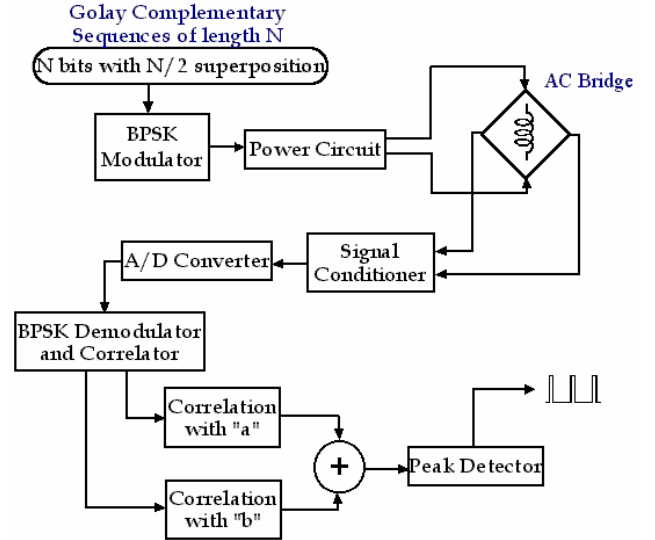


Fig. 6: Block diagram of the system.

When the wheel of the train is above of a pair of coils, the flux in the receiving coil is attenuated in an order of magnitude of 10, about 20 dB, like it was demonstrated previously. Then appears a differential voltage in the bridge, which it is digitalized by the ADC, demodulated by the BPSK demodulator, and processed by the double correlator and the peak detector. The two pairs of emitter (Tx) and receiver (Rx) coils are placed in the rail line in points between two stations (fig. 7) or next to junctions or bifurcations. In fig. 8 and 9 it can see the results of the signal process using a codification made with Golay complementary sequences of length $N=32$ bits, without noise, and supposing a train circulating between “x” and “y” station (in both directions). As it can be seen, the sense of circulation of the train is determined checking the polarity of the correlation peaks.

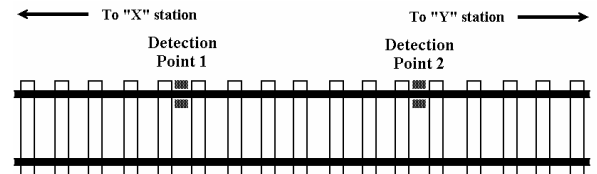


Fig. 7: Ubication of the coils in the rail

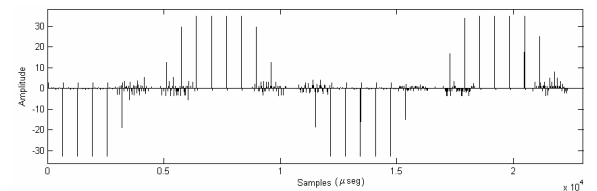


Fig. 8: Wheel train detected circulating from X to Y.

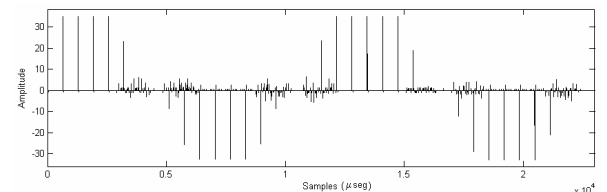


Fig. 9: Wheel train detected circulating from X to Y.

In fig. 10 and 11 it can be seen the results of the detection in the same conditions of signal processing and codification, but with a SNR of -9dB .

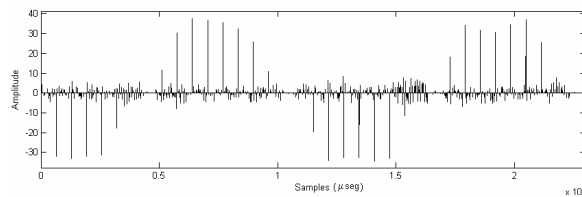


Fig. 10: Wheel train detected circulating from X to Y (SNR= -9dB).

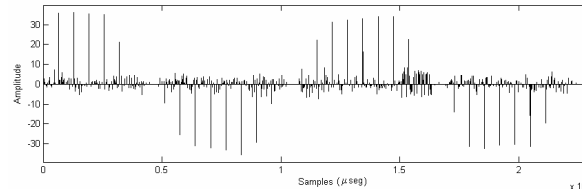


Fig. 11: Wheel train detected circulating from X to Y (SNR= -9dB).

The module of signal process has been implemented in FPGA. This is possible because all the operations of modulation and correlation are digital and are composed of sequences of binary values $\{-1; +1\}$. Due to this, all the operations are reduced to sums and subtractions (Hernández, 2002), (Popovic, 1999). The possibilities of the proposed system don't finish here. It is considered in the investigation to combine more pairs of coils, and connect all them in the same way of the fig. 5. If the coupling coefficients of all the pairs of coils are different among them, it can be determined over which couple of coils is the train wheel. This procedure can be extended for new pairs of coils defining new values for its coupling coefficient. This will be reflected in the amplitude and sign of the deltas at the output of the processing system. In fig. 12 can be seen the result of simulation considering a system with four pairs of coils: there are four different amplitudes, corresponding to four different detection points, easily detectable.

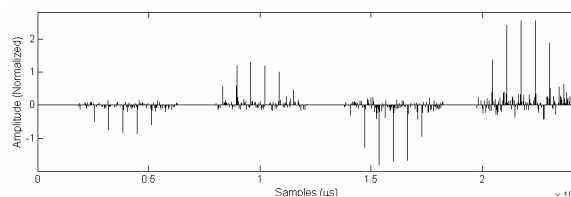


Fig. 12: Signal process results for four pairs of coils.

5. CONCLUSIONS

In this work, it has been presented an electronic wheel train detector that uses a continuous emission of coded signals to work with low SNR. This characteristic allows the placement of the sensors in the rail without "in situ" electronic signal processing. That makes easier the maintenance and control tasks, in addition to improve the robustness of the external equipment. The use of an AC bridge configuration to connect the emitter and the receiver coils improves the sensibility of the sensor and allows the detection of the sense of train circulation.

6. ACKNOWLEDGEMENTS

This work has been possible thanks to the financing of the Ministry of Science and Technology through project TELEVÍA (reference COO1999-AX049).

REFERENCES

- Anslys (2002). ANSYS 6.1 Technical documentation (Basic, Modelling, Meshing and Advance).
- Donato, P., Ureña, J., Mazo, M., García, J.J., Hernández, A. (2003a). Sistema de detección de paso de ruedas de tren sin electrónica en vía. *Seminario Anual de Automática, Electrónica Industrial e Instrumentación (SAAEI 2003)*. CD Edition. Vigo, Spain.
- Donato, P., Ureña, J., Mazo, M., García, J.J., Hernández, A. (2003b). Use of Coded Signals to Wheel Train Detection. *9th IEEE International Conference on Emerging Technologies and Factory Automation (ETFA 2003)*. ETFA 2003 Proceedings **Volume 2**, IEEE Catalog Number:03TH8696. ISBN:0-7803-7937-3, pp: 685-691. Lisbon, Portugal.
- Futsuhara, K., and Mukaidono, M. (1988). A realization of fail-safe sensor using electromagnetic induction, *Conference on Precision Electromagnetic Measurement 1988 (CPEM'88)*, CPEM'88 Digest, pp. 99-100. Tsukuba, Japan.
- Futsuhara, K. and Mukaidono, M. (1999). Realization of a fail-safe train wheel sensor using electromagnetic induction. *IEEE Transactions on Instrumentation and measurement*, **Volume 38**, No.2, pp. 421-426.
- Hernández, A., Ureña, J., García, J.J., Díaz, V., Mazo, M., Hernanz, D., Dértin, J.P., Serot, J. (2002). Ultrasonic signal processing using configurable computing, *15th Triennial World Congress of the International Federation of Automatic Control (IFAC'02)*. Barcelona, Spain.
- OPTI, Observatorio de Prospectiva Tecnológica Industrial (1999). *Cuestionario de prospectiva Tecnológica de la Industria del Ferrocarril*, Ministerio de Industria y Energía, Spain.
- Popovic B. M. (1999). Efficient Golay correlator, *IEEE Electronics letters*, Vol. 35 No. 17.
- RENFE, Mantenimiento de Infraestructura (1999). *Especificación Técnica de Suministro de Sistemas Contadores Electrónicos de Ejes*, ET03.365.310.6.
- Tseng, C.-C and Liu, C.L. (1972). Complementary Sets of Sequences. *IEEE Trans. Information Theory*, **Vol. IT-18**, No 5, pp. 644-652.
- Ureña, J., Mazo, M., García, J.J., Hernández, A., Villadangos, J., Marrón, M., Pastor, J., Escudero, M., García, R. (2001). Train axle detector based on signal codification with a Barker code, *Automotive and Transportation Technology Congress and Exhibition, ATTCE 2001*, **Volume 8**. pp. 49-53. Barcelona, Spain.